Experiments on Exploration of Shallow Fine Structures and the Construction of the 1-D Velocity Model in the Pingtan Island Fujian[1]

GUO Yang[1)]   XU Jiajun[1) 2)]   LIN Chen[1)]   JIN Xing[1)]   YAO Huajian[2)]   YANG Hongfeng[4)] and CAI Huiteng[1) 3) *]

1) Fujian Earthquake Agency   Fuzhou 350003   China
2) School of Earth and Space Sciences   University of Science and Technology of China   Hefei 230026   China
3) School of Earth Sciences and Engineering   Nanjing University   Nanjing 210046   China
4) Earth System Science Programme   Faculty of Science   The Chinese University of Hong Kong   Hong Kong 999077   China

---

112 short-period seismographs were set up in the 400km^2 area of Pingtan Island and its surrounding areas in Fujian. The combined observations of the airgun source and ambient noise source were carried out using a dense array to receive the 387 airgun signals excited around the island and one month of continuous ambient noise recording. The 1-D P-wave and S-wave shallow velocity model of Pingtan Island is obtained by the inversion of the airgun body wave's first arrival time data and the reliability of the velocity model is verified by using the surface wave phase velocity dispersion curve which can provide initial model for subsequent 3-D imaging. The experimental results show that this experiment is a successful demonstration of local scale green non-destructive detection which can provide basic data for shallow surface structure research and strong vibration simulation of the Pingtan Island.

Key words: **Pingtan Island**; **Fujian**; **Dense array**; **Airgun**; **Ambient noise**; **1-D velocity model**

INTRODUCTION

The Pingtan Island is the largest and most easterly island among the islands along the

* Corresponding author.

southeast coast of Fujian. It borders the Taiwan Strait in the east and the Haitan Strait in the west. The geographical coordinates are 25°15′−25°45′N and 119°32′−120°10′E. In 2009 Pingtan established a comprehensive experimental zone and gradually developed into the core area for the development of the Straits Economic Zone. The geological structure of Pingtan Island is shown in Fig.1. It can be seen from Fig.1 that Pingtan Island is located at the northern end of the Pingtan−Dongshan metamorphic belt. It is a typical sea−eroded landform. The terrain is dominated by plains and hills and the coastline is tortuous. The island mainly exhibits Cretaceous volcanic rocks（K_1）and Jurassic metamorphism（J_3）and Yanshanian granite（Huang Yusheng 1995; Li Wuxian 1999）. It developed a Quaternary system in the Gulf Plain and the inter−mountain depression which is a marine−continental interaction and continental deposition not integrated in the Yanshanian granites and Pre−Quaternary Strata（Fujian Institute of Geological Survey 2016）. The island only develops a NE−trending fault mainly located in the northern and central parts of Pingtan Island and belongs to the Changle−Nan′ao fault zone. The east side is the littoral fault zone and the scale of the fault is long and extensive（Huang Zhao et al. 2006）. In 1574 the M_S5.8 destructive earthquake occurred on the Pingtan section of the littoral fault zone.

At present the digital information of urban geosciences is mainly concentrated on the surface of the earth and there are few digital studies on the geological structures below the surface （Wang Weitao et al. 2018）. The construction of three−dimensional maps of the urban underground especially the construction of fine structure maps of shallow strata is of great significance for the simulation of strong urban earthquakes and the evaluation of engineering and building safety which can minimize the harm of casualties and social economy development caused by natural disasters（Chen Yong et al. 2003）. The delineation of the fine structure of the shallow crust depends on local detection whose horizontal range is usually 1−20km and the detection depth is generally about 5km from the surface to the ground. The main purpose of the research involves resource development and utilization urban underground space development and urban ground building disaster reduction and disaster prevention etc.（Chen Yong et al. 2017）. According to the type of detected source local scale detection can be divided into passive source detection and active source detection. Passive source detection is dominated by natural earthquakes and ambient noise. Although natural earthquakes have strong energy the uncontrollable factors such as the limitations of space−time distribution limit their application in local scale detection（Chen Yong et al. 2017）. In recent years the use of high−frequency surface wave ambient noise tomography to detect shallow crustal structures is widely used（Picozzi M. et al. 2009; Huang Y. C. et al. 2010; Pilz M. et al. 2012; Lin Fanchi et al. 2013; Shirzad T. et al. 2014; Fang Hongjian et al. 2015 Li Cheng et al. 2016）. In terms of active source detection considering environmental and safety factors the explosive source is no longer suitable for detecting shallow crustal structures in urban areas. When the study area is adjacent to the ocean the green large−capacity airgun source becomes an effective tool for nondestructive detection of shallow crust structures（Zollo A. et al. 2003; Evangelidis C. P. et al. 2004; Majdański M. et al. 2008; Paulatto M. et al. 2010; Shalev E. et al. 2010; Paulatto M. et al. 2012; García−Yeguas A. et al. 2012; Zhang Yunpeng et al. 2016）.

In view of this in 2018 the Fujian Earthquake Agency organized a dense array observation experiment of near−surface shallow structures in Pingtan Island. Taking the "Yanping No.2" scientific research ship as the large−capacity airgun source carrier ring of the Pingtan Island voyage type excitation operation they deployed the dense array to receive the airgun body wave signal and continuously observed the dense array for one month to obtain the ambient noise signal. It is proposed that high−resolution 3−D image of shallow fine structure be obtained by means of joint imaging of the active source and passive source so as to achieve the goal of constructing a 3−D underground map of the Pingtan comprehensive experimental area. This paper

mainly summarizes and introduces the observation system　data processing and preliminary construction of the shallow 1-D velocity model of this experiment　and provides basic data for the subsequent three-dimensional research work.
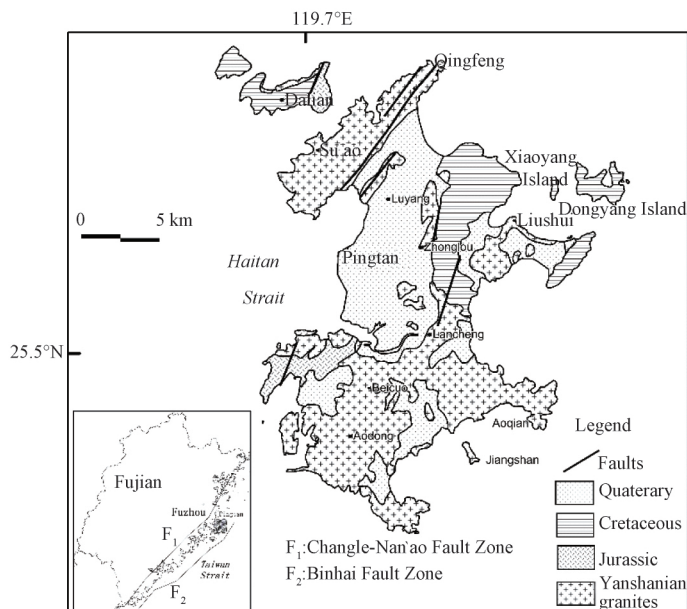

Fig.1　The Pingtan geological map

1　EXPERIMENT

This experiment uses the Pingtan Island dense array to carry out joint observations of airgun and ambient noise. Fig.2 is the observation system diagram　in which the red pentagram is the Pingtan Island dense array and the blue line is the sea navigation survey line.

The Pingtan Island dense array consists of 112 portable seismographs QS－05A－1（5s ~ 250Hz）. The sampling rate of the instrument is 100Hz　which is evenly distributed throughout the Pingtan Island and surrounding area　where the average station spacing is approximately 2km. In order to ensure the reliability of the final data acquisition　the array layout includes the previous array design　point survey and consistency test　as well as subsequent field layout　inspection rotation and recycling instruments. Considering the factors such as the tightness of the seal and the convenience of the rotation of the instrument　the waterproof cover sleeve is designed independently. When the layout is set　the sleeve is placed in the pit and compacted　and then the instrument is placed in the sleeve for horizontal alignment　north adjustment and clock adjustment　etc.　it is finally buried in the soil layer and realizes the process layout.

The airgun source consists of six 1500 LL bolt airgun array with a total volume of 12　000in^3（Jin Zhen et al.　2018）. The "Yanping No.2" scientific research ship circle Pingtan Island escaping the sea to excite the airgun signal. Among them　the PT01 line near the island has a total of 195 shots. The length of the route is 47. 33km　the average gun spacing is 244m. And the PT02 line far from the island　a total of 192 shots were excited　with a length of 47. 55km and an average shot spacing of 249m. The ambient noise data is waveform records obtained by successive observations of the dense array for one month.
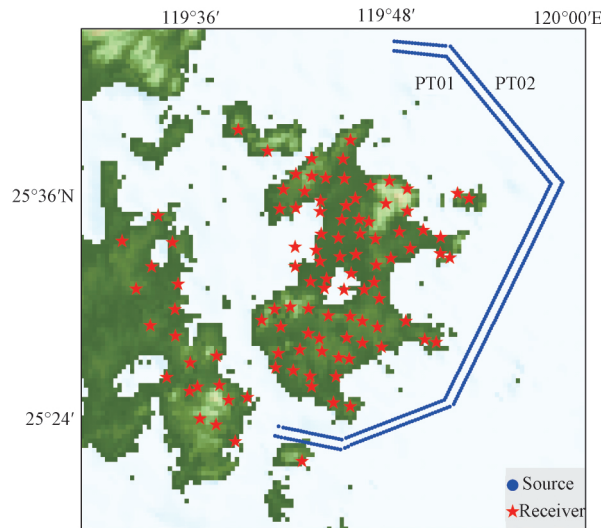
Fig.2 Observing system

2   DATA PROCESSING

2.1   Airgun Source Data

Firstly the airgun waveform data is derived from the SD card of the portable seismograph. In the form of a common receiving point the waveform data of $-20-120$s is intercepted according to the airgun excitation time and converted into an international common SEGY format and stored in the database. Before the seismic phase picking the profile is de-trending de-mean phase-free digital filter 3－7Hz filtering and normalization pre-processing (Xu Jiajun et al. 2016).

The common receiving point profile is drawn according to the reduced velocity (6km/s) to obtain a P-wave Z-channel recording sectional view wherein Fig.3(a) is the P054 station on the PT01 line and Fig.4(a) is the P103 station around the PT02 line. According to the characteristics of the seismic phase through the phase comparison and analysis the first arrival Pg phase can be clearly identified by using the chase record. The Pg phase is a refraction wave from the crystalline basal layer. The energy in the near field is strong and the phase is continuous which can be continuously tracked. However limited by the offset of the observing system it is only traced to about 45km. As can be seen from the cross-sectional view (Fig.3(a) Fig.4(a)) the Pg phase reduced travel time curve is parallel to the X-axis as a whole indicating that its average apparent velocity is close to the reduced velocity(6km/s). However at 24－27km and 27－33km the reduced travel time shows obvious hysteresis compared the positions of the two sides that is the local velocity structure is different. From the scatter plot of the Pg(Fig.5(a)) it can be seen that the 22629 Pg phases picked up are relatively concentrated the reduced travel time is between 0.07－0.70s and the average reduced travel time is 0.33s.

The common receiving point profile is drawn at the reduced velocity (3.46km/s) to obtain a cross-sectional view of the S-wave Z-channel recording (Fig.3(b) Fig.4(b)). As can be seen from the cross-sectional view the S-wave energy is significantly weaker than the P-wave compared to the P-wave. Similar to the P-wave the farthest offset is about 45km and the travel time curve is parallel to the X axis. The reduced travel time is also relatively delayed at 24－27km and

27−33km.From the scatter plot of the Sg(Fig.5(b)) it can be seen that the 21532 Sg phases picked up are relatively concentrated the reduced travel time is between 0.00−0.70s and the average reduced travel time is 0.35s.
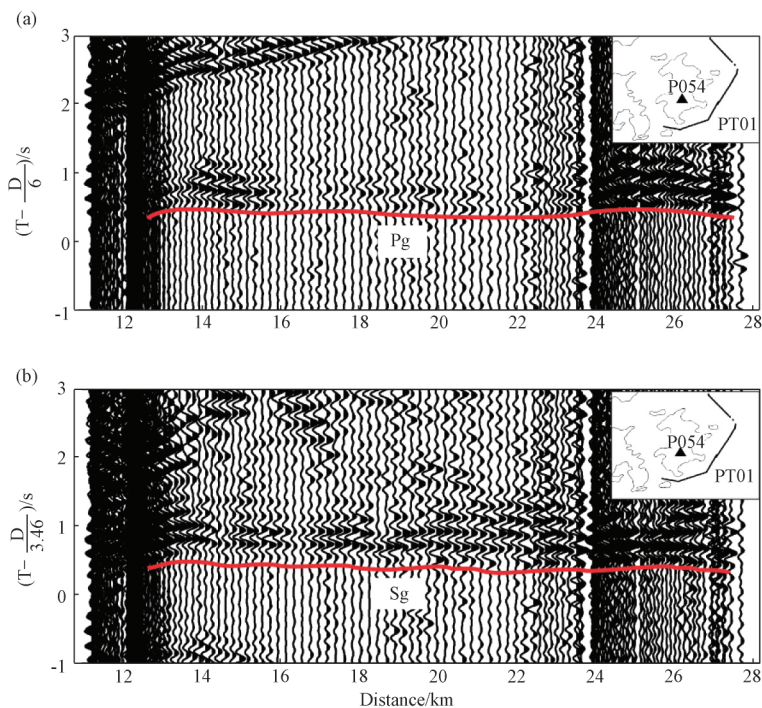

Fig 3 Recorded section and first arrival phase of P054 station in PT01 line
(a) Reduced velocity 6km/s.(b) Reduced velocity 3.46km/s

2.2 Ambient Noise Source Data

First re‑sampling de‑mean de‑trending band‑pass filtering time domain normalization and spectral whitening are performed on the daily vertical component waveform data of each station in the array. The ambient noise is cross‑correlated in the same time period at each station pair and the results of one month are superimposed to obtain the Rayleigh surface wave empirical Green's function with high signal‑to‑noise ratio at each station pair (Fig.7).

3 SHALLOW 1‑D VELOCITY MODEL

3.1 Model Construction

Using the picked Pg and Sg airgun travel time data the shallow surface velocity and corresponding depth of the study area are given according to the WH method travel time inversion calculation (Department of Scientific Programming and Earthquake Monitoring SSB 1988; Wang Shuaijun et al. 2007; Li Pei et al. 2015) to obtain the 1‑D P‑wave and S‑wave shallow velocity model in the region and the corresponding wave velocity ratio and Poisson's ratio (Fig. 8). The wave velocity ratio ranges from 1.64 to 1.73 the Poisson's ratio is between 0.20 and 0.25 and the average Poisson's ratio is 0.23. It can be seen from the fitting effect diagrams of P‑wave and S‑wave (Fig.5 Fig.6) that the theoretical travel time curve is close to the average
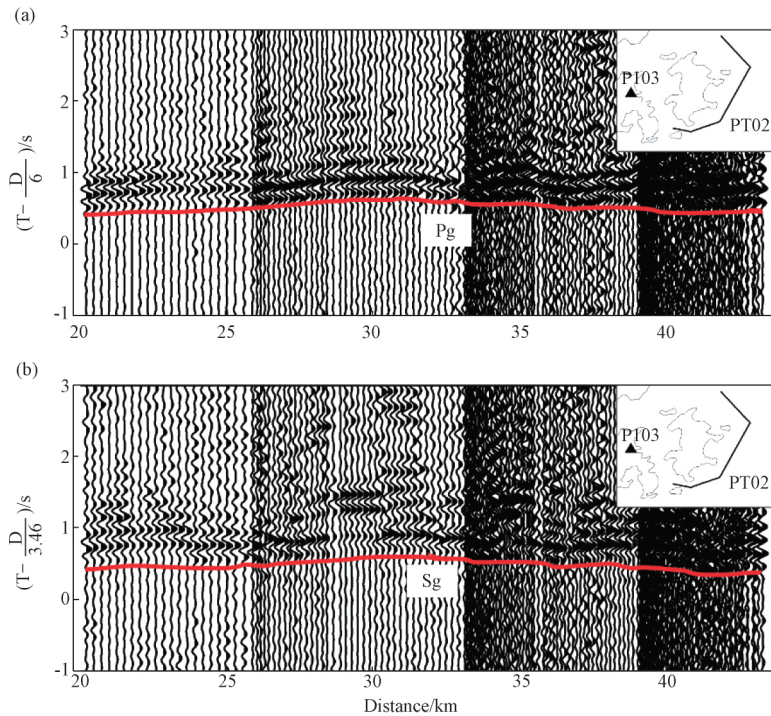
Fig.4   Recorded section and first arrival phase of P103 station in PT02 line
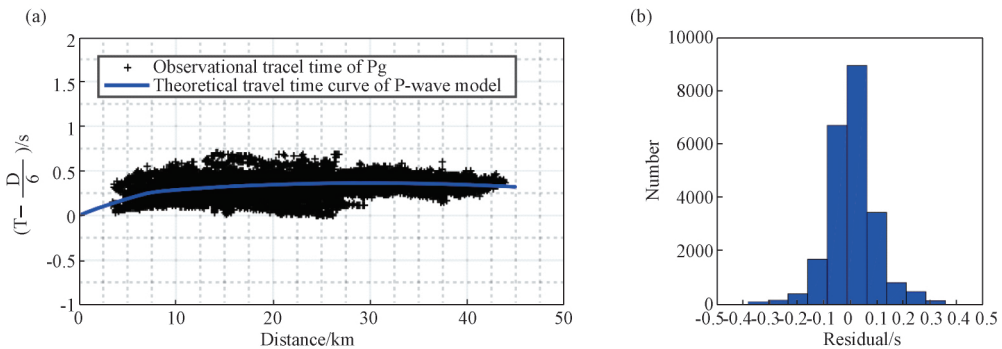（a）Reduced velocity 6km/s.（b）Reduced velocity 3. 46km/s

Fig.5   Fitting effect of Pg phase travel time
（a）Travel time of seismic phase and fitting curve.（b）Histogram of residual distribution

distribution of observation values　and the Pg and Sg travel time residuals are 0. 08s and 0. 11s respectively. The travel residual distribution approximates a normal distribution.

3. 2   Surface Wave Verification

According to the velocity model　the depth-sensitive kernels of the phase velocity of the fundamental Rayleigh surface wave with different periodicity can be obtained（Fig.9）. It can be seen from the Figure that the dispersion of the surface wave mainly depends on S-wave velocity. The longer the period　the deeper the sensitivity depth　and the shallow portion is equally sensitive to P-wave and density in a short-period.
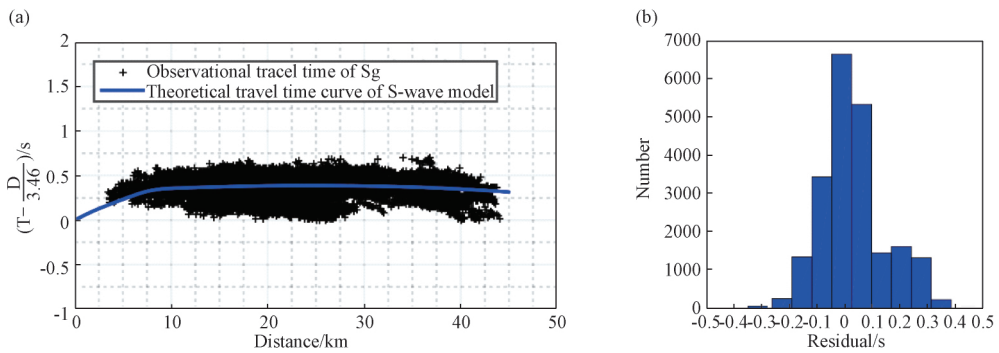
Fig.6　Fitting effect of Sg phase travel time
（a）Travel time of seismic phase and fitting curve （b）Histogram of residual distribution

　　The theoretical phase velocity dispersion curve of the velocity model is then calculated and compared with the actual average phase velocity dispersion curve. As can be seen from Fig.10 the degree of agreement between the two is higher. Therefore　the reliability of the Pingtan shallow 1-D velocity model obtained in this paper is verified to be high.
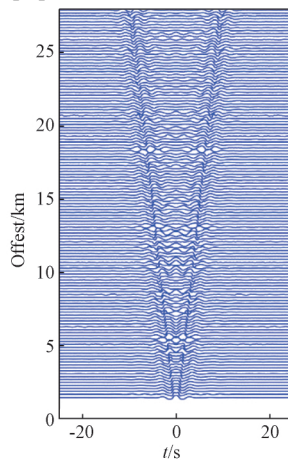

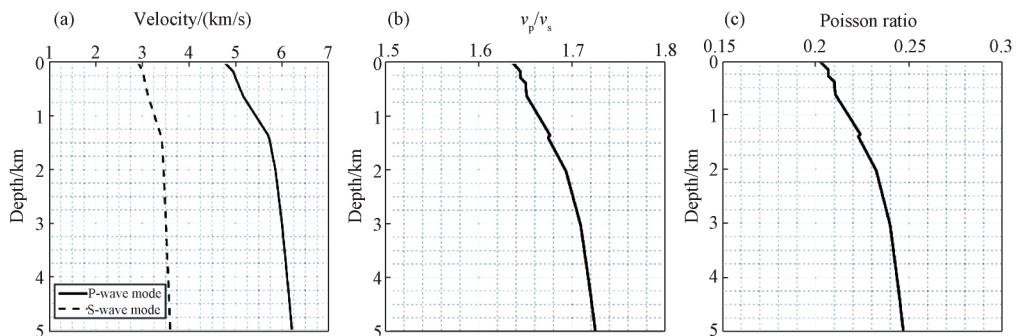**Fig.7**　Rayleigh wave experience Green's function

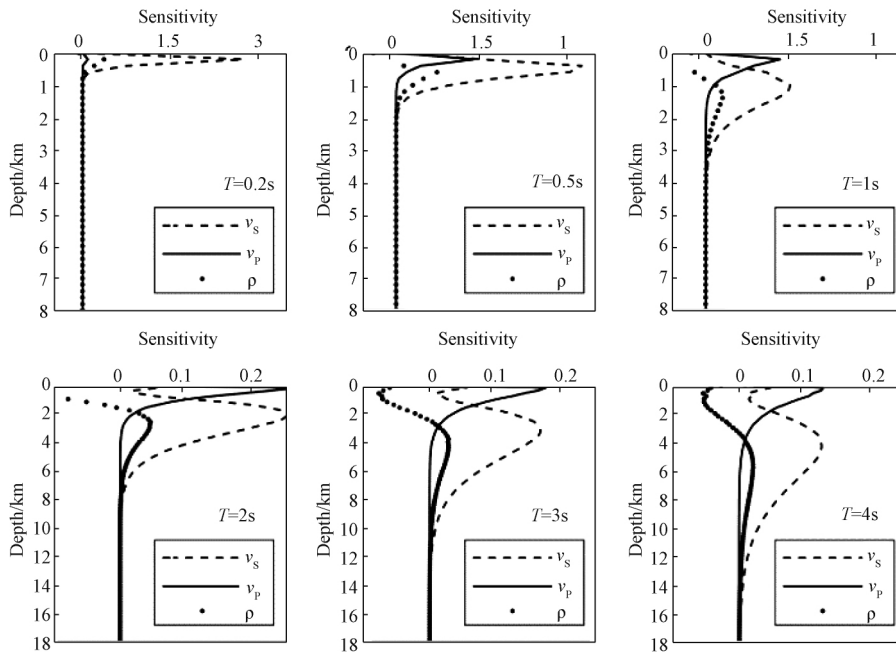**Fig.8**　P-wave and S-wave velocity model　wave velocity ratio and Poisson's ratio

Fig.9　Deep-sensitive kernels of P-wave and S-wave velocity and density for fundamental
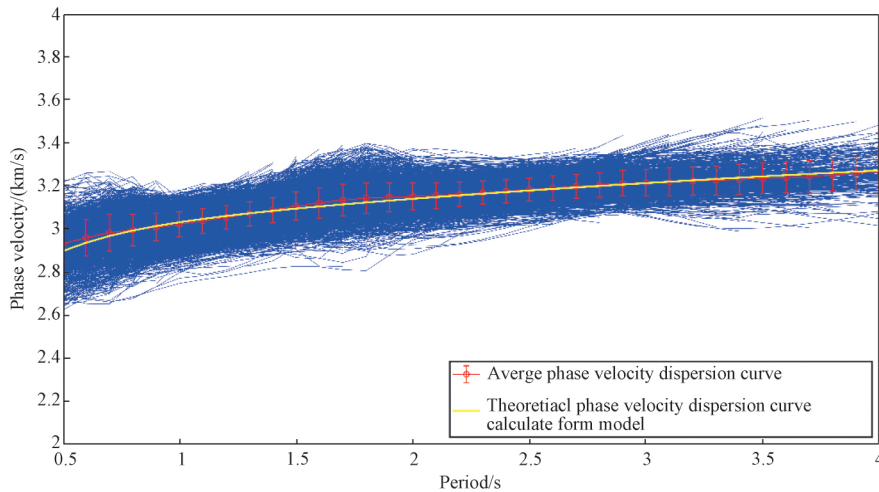Rayleigh wave velocity in different periodic

Fig.10　Fundamental Rayleigh wave phase velocity dispersion curve

3　DISCUSSION

　　The body wave shallow velocity of the study area is relatively high　which is similar to the
results of Cai Huiteng et al. (2015) and Chen Kaixun et al. (2016). It is believed that the upper
crust of the Pingtan-Dongshan metamorphic belt in Fujian is at a high-velocity anomaly　and it is
assumed that the Quaternary sedimentary strata in the area are relatively thin or the crystallization

depth of the crystalline base is shallow　which may be related to the volcanic eruption and magma intrusion and the crustal uplift in the area　leading to large areas of volcanic rocks and granite exposure. The overall Poisson's ratio of the upper crust in the study area is low（all less than 0. 25）　which may be due to the study area located in the South China continental margin orogenic belt. Under the action of orogenic movement　the crustal movement forms the Pingtan–Dongshan shear tectonic belt（Cui Jianjun et al.　2013）　it is speculated that the composition of the continental crust is transformed into granite‑based　and the upper crust may be a long‑ying acidic　medium‑acid rock（Huang Hui et al.　1990）.

4　CONCLUSION

In this paper　from the high‑volume　high‑quality observation data obtained from the shallow surface fine structure detection experiment of Pingtan Island in Fujian　the Pingtan average 1‑D shallow velocity model was obtained based on the body wave data　and the reliability was verified by surface wave data　which provides a reliable initial model for subsequent three‑dimensional high‑precision imaging in this area.

Fine detection of urban shallow surface by green non‑destructive detection is helpful to construct a three‑dimensional map of the urban shallow underground　which is of great significance to the utilization of urban underground space　the simulation of strong earthquakes and the risk assessment of earthquake disasters. The Pingtan Island shallow fine structure detection experiment is the first attempt in China to detect urban shallow fine structures based on a dense array combined airgun source and ambient noise source at the urban scale. The success of the detection experiment has a demonstrative effect on promoting similar work.

REFERENCES

Cai Huiteng　Kuo‑Chen H.　Jin Xin　Wang C.Y.　Huang B.S.　Yen H.Y. A three‑dimensional Vp　Vs　and Vp/Vs crustal structure in Fujian　Southeast China　from active‑ and passive‑source experiments　J　. *Journal of Asian Earth Sciences*　2015　111: 517−527.

Chen Kaixun　Kuo‑Chen H.　Brown D.　Li Qiusheng　Ye Zhuo　Liang W.T.　Wang C.Y.　Yao Huajian. Three‑dimensional ambient noise tomography across the Taiwan Strait: the structure of a magma‑poor rifted margin　J　. *Tectonics*　2016　35（8）: 1782−1792.

Chen Yong　Chen Longsheng　Yu Sheng. Urban geophysics: a new discipline of earth science　J　. *Journal of Geodesy and Geodynamics*　2003　23（4）: 1−4（in Chinese with English abstract）.

Chen Yong　Wang Baoshan　Yao Huajian. Seismic airgun exploration of continental crust structures　J　. *Science China Earth Sciences*　2017　60（10）: 1739−1751.

Cui Jianjun　Zhang Yueqiao　Dong Shuwen　Jahn B.M.　Xu Xianbing　Ma Licheng　Li Jianhua　Su Jinbo　Li Yong. Late Mesozoic orogenesis along the coast of Southeast China and its geological significance　J　. *Geology in China*　2013　40（1）: 86−105（in Chinese with English abstract）.

Department of Scientific Programming and Earthquake Monitoring　SSB. *Developments in the Research of Deep Structures Chinese' Continent*　M　. Beijing: Geological Publishing House　1988: 19−46（in Chinese）.

Evangelidis C.P.　Minshull T.A.　Henstock T.J. Three‑dimensional crustal structure of Ascension Island from active source seismic tomography　J　. *Geophysical Journal International*　2004　159（1）: 311−325.

Fang Hongjian　Yao Huajian　Zhang Haijiang　Huang Y.C.　Van Der Hilst R.D. Direct inversion of surface wave dispersion for three‑dimensional shallow crustal structure based on ray tracing: methodology and application　J　. *Geophysical Journal International*　2015　201（3）: 1251−1263.

Fujian Institute of Geological Survey. *Regional Geology of China　Fujian Province*　M　. Beijing: Geological Publishing House　2016: 681−683（in Chinese）.

García‑Yeguas A.　Koulakov I.　Ibáñez J.M.　Rietbrock A. High resolution 3D P wave velocity structure beneath Tenerife Island（Canary Islands　Spain）based on tomographic inversion of active‑source data　J　. *Journal of Geophysical Research*: *Solid Earth*　2012　117（B9）: B09309.

Huang Hui　Li Rongan　Yang Chuanxia. Geochronologic study for the metamorphic belt along the coast of Fujian

Province and its tectonic significance〔J〕. *Chinese Science Bulletin*，1990，35(9)：751−754.

Huang Y.C.，Yao Huojian，Huang B.S.，Van Der Hilst R.D.，Wen Kuoliang，Huang W.G.，Chen C.H. Phase velocity variation at periods of 0.5−3 seconds in the Taipei basin of Taiwan from correlation of ambient seismic noise〔J〕. *Bulletin of the Seismological Society of America*，2010，100(5A)：2250−2263.

Huang Zhao，Wang Shanxiong. Tectonic features and activity of Binhai fault zone in Taiwan strait〔J〕. *Journal of Geodesy and Geodynamics*，2006，26(3)：16−22 (in Chinese with English abstract).

Huang Yusheng，Cai Chuanrong，Zhou Hong. Geochemistry of amphibole dacite Series in Pingtan，Fujian〔J〕. *Geology-Geochemistry*，1995(1)：62−67 (in Chinese).

Jin Zhen，Li Shanyou，Cai Huiteng，Li Pei，Li Haiyan，Xu Jiajun. 3D P−wave velocity structure of crust in Fujian and the southern Taiwan Strait derived from air-gun seismic data〔J〕. *Chinese Journal of Geophysics*，2018，61(7)：2776−2787 (in Chinese with English abstract).

Li Cheng，Yao Huajian，Fang Hongjian，Huang Xianliang，Wan Kesong，Zhang Haijiang，Wang Kangdong. 3D near-surface shear-wave velocity structure from ambient-noise tomography and borehole data in the Hefei Urban Area，China〔J〕. *Seismological Research Letters*，2016，87(4)：882−892.

Li Pei，Jin Xin，Wan Shanxiong，Cai Huiteng. Crustal Velocity structure of the Shaowu−Nanping−Pingtan transect through Fujian from deep seismic sounding-tectonic implications〔J〕. *Science China Earth Sciences*，2015，58(12)：2188−2199.

Li Wuxian，Dong Chuanwan，Zhou Xinmin. Plagioclase xenocryst and magma mingling in Pingtan and Zhangzhou complexes〔J〕. *Acta Petrologica Sinica*，1999，15(2)：286−290 (in Chinese with English abstract).

Lin Fanchi，Li Dunzhu，Clayton R.W.，Hollis D. High-resolution 3D shallow crustal structure in Long Beach，California：application of ambient noise tomography on a dense seismic array〔J〕. *Geophysics*，2013，78(4)：Q45−Q56.

Majdański M.，Środa P.，Malinowski M.，Czuba W.，Grad M.，Guterch A.，Hegedüs E. 3D seismic model of the uppermost crust of the admiralty bay area，king George island，West Antarctica〔J〕. *Polish Polar Research*，2008，29(4)：303−318.

Paulatto M.，Minshull T.A.，Baptie B.，Dean S.，Hammond J.O.S.，Henstock T.，Kenedi C.L.，Kiddle E.J.，Malin P.，Peirce C.，Ryan G.，Shalev E.，Sparks R.S.J.，Voight B. Upper crustal structure of an active volcano from refraction/reflection tomography，Montserrat，Lesser Antilles〔J〕. *Geophysical Journal International*，2010，180(2)：685−696.

Paulatto M.，Annen C.，Henstock T.J.，Kiddle E.，Minshull T.A.，Sparks R.S.J.，Voight B. Magma chamber properties from integrated seismic tomography and thermal modeling at Montserrat〔J〕. *Geochemistry Geophysics Geosystems*，2012，13(1)，doi: 10.1029/2011GC003892.

Picozzi M.，Parolai S.，Bindi D.，Strollo A. Characterization of shallow geology by high-frequency seismic noise tomography〔J〕. *Geophysical Journal International*，2009，176(1)：164−174.

Pilz M.，Parolai S.，Picozzi M.，Bindi D. Three-dimensional shear wave velocity imaging by ambient seismic noise tomography〔J〕. *Geophysical Journal International*，2012，189(1)：501−512.

Shalev E.，Kenedi C.L.，Malin P.，Voight V.，Miller V.，Hidayat D.，Sparks R.S.J.，Minshull T.，Paulatto M.，Brown L.，Mattioli G. Three-dimensional seismic velocity tomography of Montserrat from the SEA-CALIPSO offshore/onshore experiment〔J〕. *Geophysical Research Letters*，2010，37(19)：L00E17.

Shirzad T.，Hossein Shomali Z. Shallow crustal structures of the Tehran basin in Iran resolved by ambient noise tomography〔J〕. *Geophysical Journal International*，2014，196(2)：1162−1176.

Wang Shuaijun，Zhang Xiankang，Zhang Chengke，Wang Fuyun，Zhao Jinren，Zhang Jianshi，Liu Baofeng，Pan Suzhen，Gai Yujie. 2−D crustal structures along Wuqing−Beijing−Chicheng deep seismic sounding profile〔J〕. *Chinese Journal of Geophysics*，2007，50(6)：1769−1777 (in Chinese with English abstract).

Wang Weitao，Wang Baoshan，Jiang Shengmiao，Hu Jiupeng，Zhang Yuansheng. Regional scale seismological investigation on the continent crust using airgun sources—a perspective review〔J〕. *Earthquake Research in China*，2018，32(3)：315−329.

Xu Jiajun，Cai Huiteng，Jin Xing，Wang Shanxiong，Xia Ji，Li Pei. Signal detection of large volume airgun source excitation in the fixed field of the Yangtze River〔J〕. *Earthquake Research in China*，2016，30(3)：418−429.

Zhang Yunpeng，Wang Baoshan，Wang Weitao，Xu Yihe. Preliminary results of tomography from permanent stations in the Anhui airgun experiment〔J〕. *Earthquake Research in China*，2016，30(3)：405−417.

Zollo A.，Judenherc S.，Auger E.，D'Auria L.，Virieux J.，Capuano P.，Chiarabba C.，De Franco R.，Makris J.，Michelini A.，Musacchio G. Evidence for the buried rim of Campi Flegrei caldera from 3−D active seismic

imaging　J　．*Geophysical Research Letters*　2003　30(19)：2002.

About the Author

　　GUO Yang　born in 1988　is an assistant engineer at Fujian Earthquake Agency. She is mainly engaged in seismic observation　active source detection and other aspects of research. E-mail：guoyangfz@ 163.com

　　Corresponding Author：CAI Huiteng　born in 1982　is a senior engineer at Fujian Earthquake Agency. He is mainly engaged in active source detection data processing and interpretation work. E-mail：caihuiteng@ 126.com